Catalysis Today 141 (2009) 349–354

Contents lists available at ScienceDirect

Catalysis Today

journal homepage: www.elsevier.com/locate/cattod

Gold supported on Mg, Al and Cu containing mixed oxides: Relation between surface properties and behavior in catalytic aerobic oxidation of 1-phenylethanol

Peter Haider, Jan-Dierk Grunwaldt, Alfons Baiker *

Institute for Chemical and Bioengineering, Department of Chemistry and Applied Biosciences, ETH Zürich, Hönggerberg, HCI, CH-8093 Zürich, Switzerland

ARTICLE INFO

Article history:
Available online 16 July 2008

Keywords:
Gold
Aerobic oxidation
1-Phenylethanol
Surface basicity
CO_2-adsorption
Retroaldolisation
ATR-IR
Mg–Al–Cu mixed oxides
Surface carbonates

ABSTRACT

Aerobic oxidation of 1-phenylethanol was investigated over Au deposited on flame-derived Mg–Al and Cu–Mg–Al mixed oxides with different metal ratios. A maximum in acetophenone (1-phenyl-ethanone) yield was observed for catalysts based on both Cu–Mg–Al and Mg–Al mixed oxides depending on their composition. Special attention was given to the elucidation of the role of surface basicity and the influence of the preparation route on the particle size of Au. Adsorption of CO_2 from the liquid phase combined with *in situ* ATR-IR and modulation excitation spectroscopy (MES) was applied to investigate differences in the surface properties of the mixed oxides as a function of the composition. Monodentate and bidentate carbonates were identified, the former being dominant on supports with high Cu contents. In order to obtain a rough quantification of the surface basicity, the retroaldolisation of 4-hydroxy-4-methyl-2-pentanone (diacetone alcohol, DAA) was chosen as a probe reaction indicating that a ratio Mg/Al = 3 results in optimal surface basicity. Moreover, the addition of Cu only lead to a partial loss in retroaldolisation activity, indicating that also the copper sites form basic centers on the surface, however, slightly weaker ones than the corresponding Mg sites. The preparation routes applied (adsorption of colloid, deposition precipitation, and impregnation) lead to different gold particle sizes characterized by mean diameters of ≈2, ≈9 and ≈30 nm, respectively. Catalytic tests using $Au/Cu_1Mg_2Al_1O_x$ catalysts with different mean gold particle size hint towards a particle size dependence of the aerobic oxidation of 1-phenylethanol, showing higher activity for the catalyst containing gold particles of ca. 9 nm compared to those with 2 and 30 nm particles, respectively.

1. Introduction

Gold had since long been used industrially as a promoter, e.g. in the gas phase synthesis of vinyl acetate monomer in the form of supported PdAu catalysts [1–5] as well as in hydrogenation reactions [6–8]. However, it took the pioneering work of Haruta et al. [9] to boost the application of gold [10] in catalysis. Today gold-based catalysts are successfully used in various heterogeneous and homogeneous reactions as evidenced by several reviews [11–14]. Starting with the oxidation of diols [15], Au has been successfully employed in the aerobic catalytic oxidation of various structurally different alcohols at ambient and high pressure [16–23] reaching similar TOF values compared to Pd [24]. Key parameters affecting the activity of the catalyst are the oxidation state of the active Au species, for example in the catalytic oxidation of CO [12,13,25–32], the support and modifications thereof [33–38], and the influence of the Au particle size [39–43].

Recently we have reported on the strong enhancement of activity in gold-based aerobic alcohol oxidation by the concerted effect of Cu and Mg containing mixed oxide supports [22] with hydrotalcite-like composition [44]. In order to analyze the crucial structural properties, several different mixed oxide supports including Cu, Mg and Al oxides in different ratios have been prepared and tested as supports for Au in the catalytic aerobic oxidation of various alcohols.

Here we have extended this study, including a broader range of mixed Cu–Mg–Al oxide support compositions as well as CeO_2 [21] and TiO_2 [18,19] for comparison. Particular attention is given to the investigation of the basic surface properties of these catalysts and their influence on the catalytic behavior.

For this purpose, we applied CO_2 adsorption measurements from the liquid phase using ATR-IR combined with modulation excitation spectroscopy (MES) and phase sensitive detection (PSD) [45–48]. The application of MES and PSD leads to improved spectral resolution and distinction of the different surface species (carbonates). Additionally, the basicity of the Cu–Mg–Al mixed oxide supports was tested using the retroaldolisation of diacetone alcohol [49–51] as a probe reaction. Both investigations indicated that the

* Corresponding author.
E-mail address: baiker@chem.ethz.ch (A. Baiker).

0920-5861/$ – see front matter © 2008 Elsevier B.V. All rights reserved.
doi:10.1016/j.cattod.2008.06.003

Cu content as well as the (Cu + Mg)/Al molar ratio are the crucial factors influencing the surface basicity. Finally, some preliminary test of the effect of the Au particle size on the catalytic behavior using three different preparation routes for the mixed oxide-supported gold particles, a colloidal route [25,52], deposition precipitation [53] and conventional impregnation revealed that small gold particles (2 nm) are less active than larger ones (9 nm).

2. Experimental

2.1. Preparation of supports and catalysts

The ternary $Cu_aMg_bAl_cO_x$ – and the binary $Mg_bAl_cO_x$ and $Cu_aAl_cO_x$ – mixed oxide supports[1] as well as the MgO_x and the Al_2O_3 supports were prepared by flame spray pyrolysis (FSP). The designation $Cu_aMg_bAl_cO_x$ with the subscripts *a*, *b*, and *c* refers to a molar ratio of Cu:Mg:Al = *a*:*b*:*c* and is used throughout the manuscript. A series of supports have been prepared varying the (Mg + Cu)/Al ratio from 1:0 in four steps to 0:1 and varying the Cu content at a constant (Mg + Cu)/Al ratio. A detailed description of the experimental setup and the procedure applied in the preparation of the supports and of the catalysts prepared by the deposition precipitation technique can be found in [22,54,55]. Reference supports applied were CeO_2 (MCT Microcoating Technologies) and TiO_2 (P25, Degussa). For the incipient wetness impregnation, 990 mg of the support were taken and mixed with the appropriate volume of a $HAuCl_4{\cdot}3H_2O$ stock solution and dried overnight at room temperature. The catalyst was then dried at 80 °C over night and subsequently calcined at 400 °C for 3 h [18,26,56]. The calcination temperature was set to the relatively high temperature 400 °C in order to create a catalyst with larger particles than prepared by deposition precipitation and to avoid Au leaching [56]. In another preparation route, Au colloids were deposited on a Cu–Mg–Al mixed oxide support according to a recipe previously published by our group [25,52]. All glasswares used in this preparation were cleansed exhaustively and the preparation was conducted following the procedure described in detail in [25,52]. The nominal Au content of all catalysts examined here was 1 wt.%. Blank experiments performed with the pure supports showed negligible activity (yield <1%).

2.2. Retroaldolisation of 4-hydroxy-4-methyl-2-pentanone (diacetone alcohol, DAA)

The decomposition of DAA was chosen as a probe reaction for the surface basicity of the catalytic systems. The reaction was carried out at 80 °C (refluxing cylcohexane) in a 50 ml round flask using 50 mg of the support material and a solution of DAA with a concentration of 1 mol/l in cyclohexane; tetradecane was added as an internal standard. Samples were taken at different reaction times and analyzed by means of gas chromatography (Thermo Quest Trace 2000 equipped with a HP-FFAP capillary column and an FID detector). The blind test with the neat solution under the conditions given showed a conversion of <2% and was neglected in the data analysis. The reaction rate was calculated by following the conversion of diacetone alcohol with time [49,50].

2.3. Catalytic tests

Catalytic tests were performed at 90 °C using 50 mg of each catalyst and 3 mmol 1-phenylethanol in 2 ml mesitylene as a test substrate. The oxygen flow was set to 50 ml/min using mass flow controllers. O_2 was bubbled through the vigorously stirred liquid at atmospheric pressure. Samples were analyzed by gas chromatography (Thermo Quest Trace 2000 employing a HP-FFAP capillary column and FID detector); tetradecane was added as an *internal standard*.

2.4. ATR-IR spectroscopy, MES calculations

CO_2 was employed as a probe molecule to characterize the basic surface properties of the mixed oxide-supported Au catalysts. The adsorption of CO_2 leads to the formation of different carbonate species [57,58] discernible by employing ATR-IR spectroscopy and the MES approach [45–48,59]. In the MES approach, the catalytic system is modulated periodically by changing a variable of interest, e.g. concentration. If a system is perturbed with a certain frequency the affected intensities will respond at the modulation frequency (or higher harmonics thereof) and possibly exhibit a phase delay in the response [46,60], i.e. species appearing at the same time of the modulation period exhibit similar in-phase angles leading to a phase sensitive detection (PSD) of the different signals. Here, CO_2-saturated toluene was used to equilibrate the surface and subsequently, N_2-saturated and CO_2-saturated toluene were modulated. The phase-resolved spectra $A_k^{\Phi_k^{\mathrm{PSD}}}(\tilde{\upsilon})$ were then calculated from the time-resolved spectra $A(\tilde{\upsilon}, t)$ using the following equation:

$$A_k^{\Phi_k^{\mathrm{PSD}}}(\tilde{\upsilon}) = \frac{2}{T}\int_0^{\mathrm{T}} A(\tilde{\upsilon}, t)\sin(k\varpi t + \Phi_k^{\mathrm{PSD}})\,\mathrm{d}t$$

where the phase angle is denoted as Φ_k^{PSD}, the modulation period is denoted as *T* and $k\omega$ refers to the demodulation frequency with $k = 1$ being the fundamental harmonic. The measurements were performed using a Bruker Equinox 55 and an IFS 66 IR spectrometer equipped with a MCT detector and a home-made cell described in detail elsewhere [61]. The detailed description of a typical experiment can be found in [22].

2.5. Electron microscopy

STEM pictures were obtained using an electron microscope (Tecnai F30 FEI; field emission cathode, operated at 300 keV, point resolution <2 Å) equipped with a high-angle annular dark field (HAADF) detector for scanning transmission electron microscopy (STEM) and an energy dispersive X-ray (EDX) detector. This instrumentation is capable of detecting even very small metal particles (<1 nm) by Z contrast and to analyze selected points by EDX spectroscopy.

3. Results and discussion

3.1. Catalytic activity

In a previous study we have shown the importance of the Cu/Mg molar ratio in the support for the aerobic oxidation of a variety of structurally different alcohols [22]. Here we focus on the influence of the molar ratio of the divalent ions (Cu, Mg) and the trivalent Al. In agreement with our previous observations, the addition of Cu is crucial. Various catalysts have been prepared and tested in the aerobic oxidation of 1-phenylethanol to phenyl-methyl ketone, the corresponding results are depicted in Fig. 1. A broad maximum is found at specific (Cu + Mg)/Al molar ratios for the $Au/Mg_bAl_cO_x$ catalysts as well as for the $Au/Cu_aMg_bAl_cO_x$ materials. Note that the reaction on the gold catalysts supported on ternary $Cu_aMg_bAl_cO_x$ mixtures lead to higher yields compared to catalysts with a binary or single component support indicating a concerted effect of the constituents. Interestingly, the promotional effect of Cu (yield *per*

[1] Note that the support contained significant amounts of carbonates.

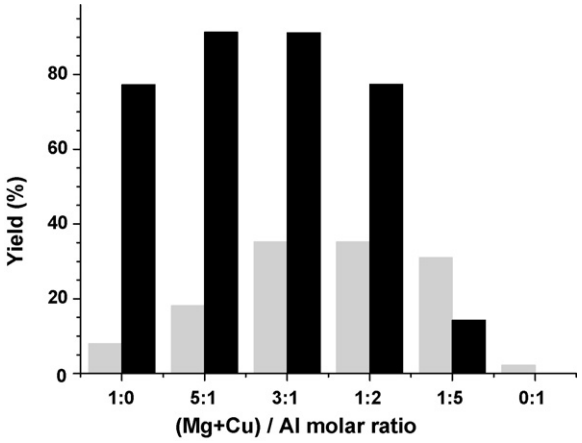

Fig. 1. Yield of acetophenone in the aerobic oxidation of 1-phenylethanol at 90 °C after a reaction time of 1 h. Conditions are specified in the experimental part. The Cu containing supports (black bars) all have an equal molar concentration of Cu and Mg. The grey bars represent the Cu-free catalysts $Au/Mg_bAl_cO_x$. The (Mg + Cu)/Al molar ratio is increasing from right to left, i.e. starting with Au/Al_2O_3, then $Au/Cu_1Mg_1Al_{10}O_x$ and $Au/Mg_1Al_5O_x$; $Au/Cu_1Mg_1Al_4O_x$ and $Au/Cu_1Mg_1Al_4O_x$ and so on.

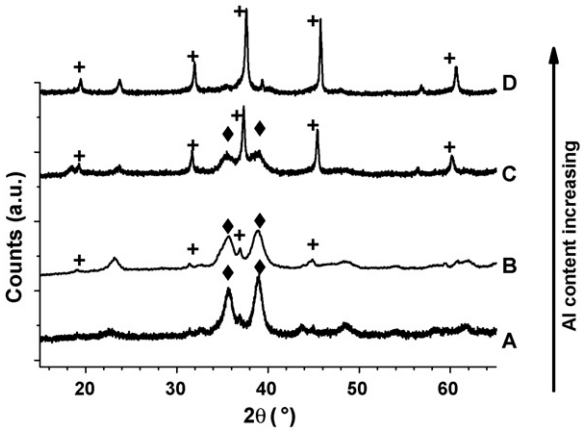

Fig. 3. XRD patterns of the catalysts with composition: $Au/Cu_5Mg_5Al_2O_x$ (A), $Au/Cu_3Mg_3Al_2O_x$ (B), $Au/Cu_1Mg_1Al_4O_x$ (C) and $Au/Cu_1Mg_1Al_{10}O_x$ (D). Pattern B is shown for comparison and has been taken from [62]. Symbols correspond to: (+) $(Mg,Cu)Al_2O_4$ spinel; (◆) CuO.

Cu added), is highest in the $Cu_1Mg_1Al_4O_x$-system having a spinel-like composition.

3.2. XRD patterns

In order to retrieve further information about the crystal phases present in the catalytic systems (Fig. 1) XRD patterns of the samples were recorded. Fig. 2 indicates that a crystalline spinel phase developed with increasing Al content, the patterns $Au/Mg_1Al_2O_x$, $Au/Mg_1Al_5O_x$ and $Au/Cu_1Mg_1Al_{10}O_x$ are hardly discernible (Figs. 2C and D and 3D). The dominating phase for the Cu containing $Au/Cu_aMg_bAl_cO_x$ catalysts is CuO (Fig. 3) which gives rise to strong reflections especially at high (Cu + Mg)/Al ratios and is still discernible in the catalyst $Au/Cu_1Mg_1Al_2O_x$. At higher Al contents a spinel phase with the general composition MAl_2O_4 is formed with M being Cu, Mg or $Cu_{(1-z)}Mg_z$.

3.3. Particle size

Gold was deposited on a ternary mixed oxide support of the composition $Cu_1Mg_2Al_1O_x$ in three different ways aiming at receiving catalysts with identical nominal composition but different Au particle size. Previously performed XANES measurements evidenced the presence of metallic gold under oxidizing reaction conditions and indicated that zero-valent gold is the active species in the catalytic dehydrogenation of alcohols [62]. The here chosen impregnation and subsequent calcinations at 400 °C (Tammann temperature 396 °C) was applied to prepare catalysts with relatively large Au particles (mean diameter ≈30 nm, Fig. 4). This catalyst only exhibited negligible activity (yield 2%). In contrast, the catalysts prepared via gold colloids [52], as well as the one prepared by deposition precipitation were highly active in the aerobic oxidation of 1-phenyalethanol to phenylmethyl ketone with yields of 73.4% (colloidal route) and 85.1% (deposition precipitation), respectively. A histogram derived from the analysis of the corresponding STEM pictures (see Fig. 5) is depicted in Fig. 4. Comparing the particles sizes (Fig. 4) it emerges that the catalysts prepared by deposition precipitation exhibited a mean particle diameter of ≈9 nm (yield 85.1%) and the catalysts prepared via the adsorption of Au colloids a mean diameter of ≈2 nm (yield 73.4%). These preliminary tests indicated that contrary to the well-established particle size effect in the oxidation of CO where small particles are much more efficient, for the aerobic oxidation of 1-phenylethanol the activity does not increase with smaller Au particles and seems to show an optimum at larger

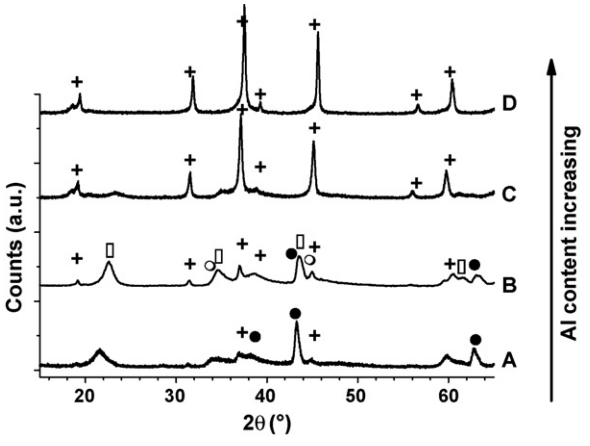

Fig. 2. XRD patterns of catalysts with different compositions: $Au/Mg_5Al_1O_x$ (A), $Au/Mg_3Al_1O_x$ (B), $Au/Mg_1Al_2O_x$ (C) and $Au/Mg_1Al_5O_x$ (D). Pattern B is shown for comparison and has been taken from [62]. The symbols correspond to: (+) spinel $(Mg,Cu)Al_2O_4$; (□) $Mg_6Al_2(OH)_{18}{\cdot}4.5H_2O$; (○) Al_2O_3; (●) MgO.

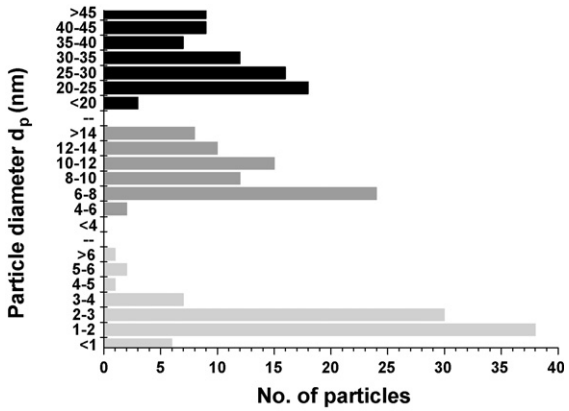

Fig. 4. Histograms of gold particle sizes resulting from different preparation methods (black: impregnated, mean size ≈30 nm; dark grey: deposition precipitation, mean size ≈9 nm; light grey: colloids, mean size ≈2.3 nm).

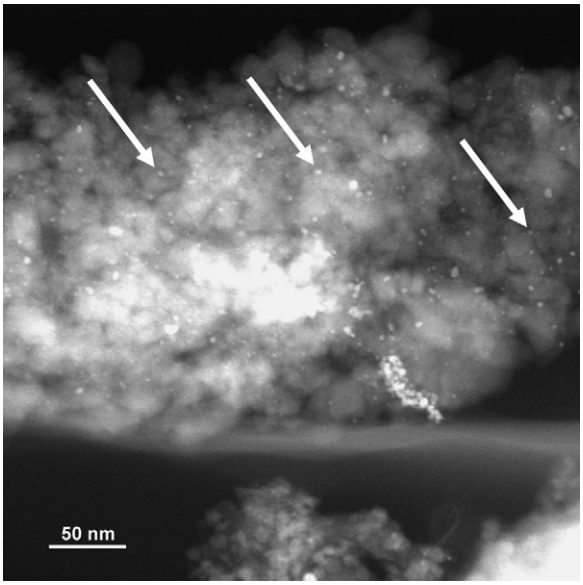

Fig. 5. HAADF-STEM images of deposited Au colloids. Note that a corresponding image of the catalyst prepared by deposition precipitation can be found in [22], the image of the impregnated catalyst is not shown. Due to the Z-contrast in the HAADF-STEM image, Au particles appear as bright spots (see arrows).

particle diameters. However, for a clearer picture of the influence of the particle diameter a more detailed study is necessary using preparation methods that allow a fine tuning of the Au particle size, ideally in a range up to 15 nm. Investigations dealing with the effect of particle size on activity and selectivity using one single preparation route leading to different, narrow particles size distributions are underway in our laboratory.

3.4. Retroaldolisation of diacetone alcohol DAA

A basic component plays a crucial role in the aerobic oxidation of alcohols [14]. The base-catalyzed retroaldolisation of DAA to acetone constitutes a test reaction that allows the semi-quantitative assessment of basic centers under reaction conditions [49–51]. In Fig. 6a, the influence of changing the molar (Cu + Mg)/Al ratios on the retroaldolisation is depicted. A significant increase in the conversion of DAA is found with increasing Mg content (Fig. 6a, black bars). However, the substitution of half the amount of Mg by Cu generally only lead to a small drop in surface basicity. Note that also for the reference materials CeO_2 and TiO_2, considerable activity in the decomposition of diacetone alcohol was observed (Fig. 6a). At a given (Cu + Mg)/Al molar ratio of 3 (Fig. 6b), the effect of the Mg/Cu molar ratio can be monitored. Again, the addition of Cu only marginally influenced the basicity of the material. Comparing the data obtained for the basic properties of the materials with the yield obtained when using these materials as supports for Au nanoparticles (Fig. 1) a similar trend, but not identical behavior is observed. It is thus suggested that surface basicity is a necessary but not sufficient prerequisite for a suitable support in the aerobic oxidation of alcohols under the given conditions.

3.5. MES ATR–IR

For a more detailed picture of the surface basicity ATR-IR experiments were performed monitoring the adsorption of CO_2 from the liquid phase on the catalysts previously studied in the retroaldolisation of DAA (Fig. 6a and b) and in the aerobic oxidation of 1-phenylethanol to phenyl-methyl ketone (Fig. 1). Additional to the conventionally recorded spectra after the adsorption of CO_2, modulation experiments were performed switching periodically from CO_2-saturated toluene to N_2-saturated toluene hence allowing a phase sensitive detection of the corresponding signals and facilitating the interpretation of the complex spectra. Au/$Mg_bAl_cO_x$ materials predominately showed signals in the regions of 1740–1600, 1325–1250 and 1000–980 cm^{-1} (Fig. 7a) assigned to carbonates bound as bidentate species similar to previous findings with Au/$Mg_3Al_1O_x$ and Au/CeO_2 catalysts [22]. A clear assignment of bands attributed to carbonate formation is achieved by comparing the corresponding in-phase angles (Fig. 7b) of all bands in the carbonate region with the in-phase angle of dissolved CO_2 (located at 2337 cm^{-1}). Note that species affected by the modulation of CO_2-saturated toluene and N_2-saturated toluene in a similar way are expected to exhibit a similar in-phase angle. Although the materials analyzed differed significantly in their composition, similar patterns were obtained (Fig. 7b). For the bands located in the regions ascribed to bidentate carbonates on Mg sites the in-phase angle of the IR peaks closely follows the in-phase angle obtained for dissolved CO_2 indicating that the spectral intensities in these regions can be attributed directly to the formation of carbonates. The Cu containing materials were analyzed in an identical manner, however, showed clear differences in the carbonates resulting from CO_2 adsorption. Predominantly on the materials with a high Cu content (Fig. 8a, graphs C and D), both bidentate and monodentate (1570–1340 and 1040–1000 cm^{-1}) carbonates were identified. Note that the modification

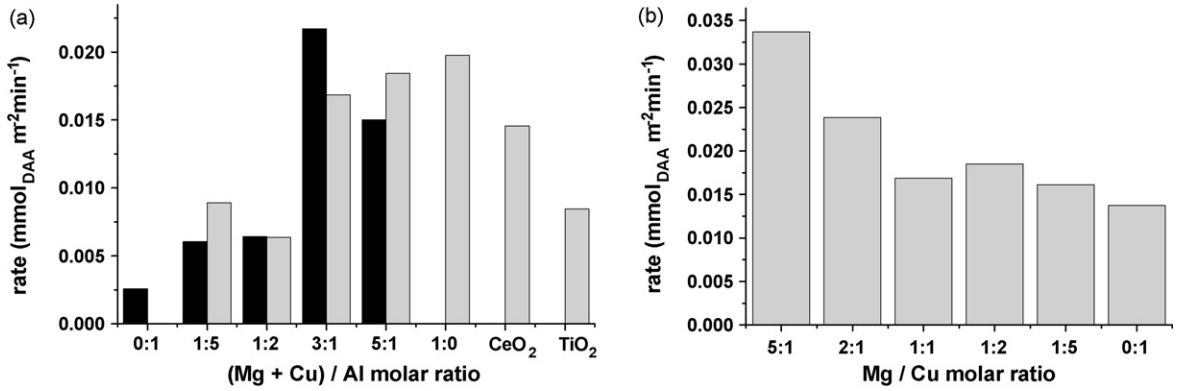

Fig. 6. (a) Rate of retroaldolisation of 4-hydroxy-4-methyl-2-pentanone (diacetone alcohol, DAA) as a function of the (Mg + Cu)/Al molar ratio (Cu containing materials: black bars, Cu-free materials: grey bars). Note that the Cu containing materials all possess a Mg/Cu molar ratio of 1, i.e. $Cu_5Mg_5Al_2O_x$, $Cu_3Mg_3Al_2O_x$, $Cu_1Mg_1Al_4O_x$ and $Cu_1Mg_1Al_{10}O_x$. (b) The rate of retroaldolisation of 4-hydroxy-4-methyl-2-pentanone (diacetone alcohol, DAA) as a function of the Cu content at a given (Mg + Cu)/Al molar ratio of 3, e.g. the sample depicted at the Mg/Cu molar ratio of 2:1 has the composition $Cu_2Mg_1Al_1O_x$.

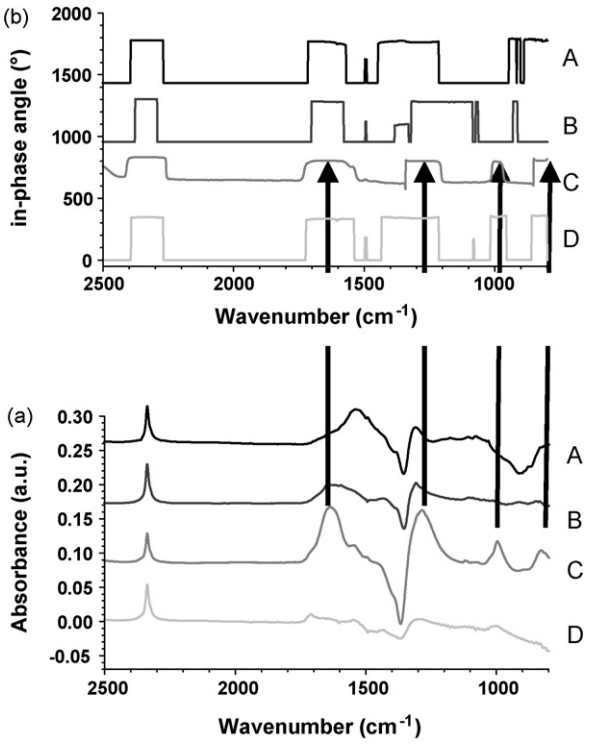

Fig. 7. (a) In-phase spectra recorded during CO_2 adsorption followed by MES ATR-IR experiments for the materials $Au/Mg_1Al_5O_x$ (A, black), $Au/Mg_1Al_2O_x$ (B, dark grey), $Au/Mg_3Al_1O_x$ (C, grey) and $Au/Mg_5Al_1O_x$ (D, light grey). Note that the pattern C was taken from [22] for comparison. (b) Corresponding graphs showing the in-phase angle Φ^{PSD}, the letter code is identical to (a). Note that species appearing at the same time of the modulation period exhibit similar in-phase angles.

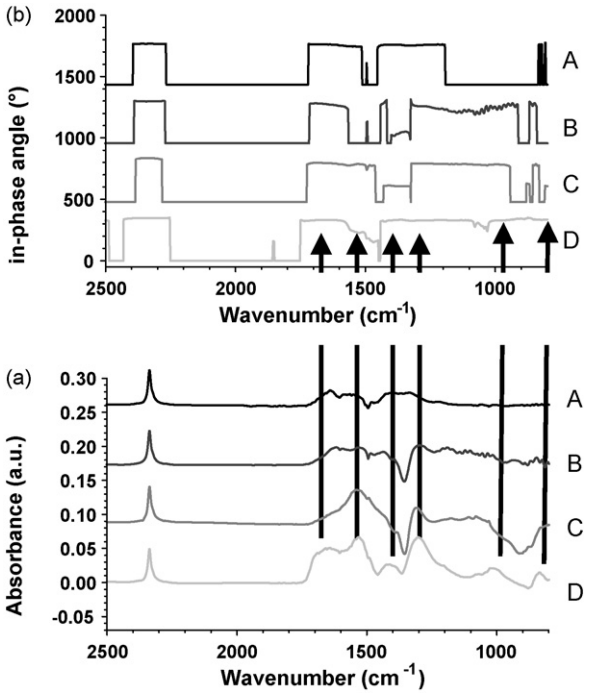

Fig. 8. (a) In-phase spectra recorded during CO_2 adsorption followed by MES ATR-IR experiments for the materials $Au/Cu_1Mg_1Al_{10}O_x$ (A, black), $Au/Cu_1Mg_1Al_4O_x$ (B, dark grey), $Au/Cu_3Mg_3Al_2O_x$ (C, grey) and $Au/Cu_5Mg_5Al_2O_x$ (D, light grey). (b) Corresponding graphs showing the in-phase angle Φ^{PSD}, the letter code is identical to (a). Note that species appearing at the same time of the modulation period exhibit similar in-phase angles.

of CeO_2 with CuO also lead to an increase in the formation of monodentate carbonates [22]. With increasing Al content (lower Cu and Mg content) the amount of monodentate carbonates decreased. Again, the corresponding in-phase Φ^{PSD} graphs clarify the presence (or absence) of monodentate carbonate species. On the sample with a high Cu content (Fig. 8b, graphs C and D), and to a lesser extent on the $Au/Cu_1Mg_1Al_4O_x$ (Fig. 8b, graph B), the in-phase angle of the spectral intensities in the region of 1570–1340 cm^{-1} resembles the in-phase angle of dissolved CO_2 indicating a direct connection of these spectral intensities. Unexpectedly, the value of the in-phase angle was also affected in the region from 1250 to 1040 cm^{-1} by the modulation experiments. However, these effects become less pronounced on the samples having a lower Cu content, the spectra and the in-phase Φ^{PSD} graphs obtained for these materials are similar to the data obtained for the corresponding Cu-free analogs. In order to extend the study from Cu–Mg–Al containing mixed oxides to single oxides, MES ATR-IR experiments were performed with Au/CeO_2 [21] and Au/TiO_2 [19] catalysts (Fig. 9a). It is observed that both samples adsorb CO_2 well, showing strong signals at ν = 1600 cm^{-1} attributed to bidentate carbonate species. However, signals are also observed in the region from 1570 to 1340 cm^{-1} as well shown in the in-phase Φ^{PSD} graphs (Fig. 9b). As observed previously for CeO_2, also TiO_2 seems to possess basic surface centers able to bind CO_2.

A comparison of the results obtained from MES ATR-IR measurements combined with phase sensitive detection of the spectral intensities with the results obtained from the retro-aldolisation of diacetone alcohol reveals interesting similarities. The higher the (Mg + Cu) content in the catalysts, the more active were the materials in the decomposition of diacetone alcohol and the more intense the carbonate IR-peaks appear in the IR spectra (Fig. 8a, graphs C and D). On the contrary, a higher Al content leads to lower conversion in the retroaldolisation of DAA. The in-phase Φ^{PSD} graphs (Fig. 8b, graphs A and B) of $Cu_1Mg_1Al_4O_x$ and

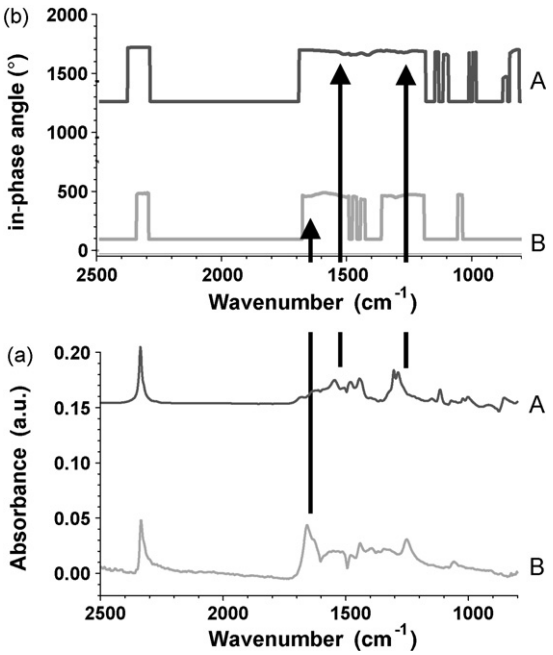

Fig. 9. (a) In-phase spectra recorded during CO_2 adsorption followed by MES ATR-IR experiments for Au/CeO_2 (A, dark grey) and Au/TiO_2 (B, light grey). (b) Corresponding graphs plotting the PSD angle Φ^{PSD}, the letter code is identical to (a). Note that species appearing at the same time of the modulation period exhibit similar in-phase angles.

$Cu_1Mg_1Al_{10}O_x$ exhibit similarity with the corresponding Cu-free analogs $Mg_1Al_2O_x$ and $Mg_1Al_5O_x$ (Fig. 7b, graphs A and B) – monodentate species are only found to a lesser extent – and also in the retroaldolisation of DAA, the differences in the basicity of $Cu_1Mg_1Al_4O_x/Mg_1Al_2O_x$ and $Cu_1Mg_1Al_{10}O_x/Mg_1Al_5O_x$ (Fig. 6a) are comparably small.

4. Conclusions

Subtle differences in the surface chemistry of flame-derived mixed oxide supports containing Cu, Mg, and Al employed as supports in the gold-catalyzed aerobic oxidation of 1-phenylethanol to phenyl-methyl ketone have been elucidated by CO_2 adsorption studies using ATR-IR and retroaldolisation of diacetone alcohol. ATR-IR spectroscopy combined with the MES approach allowed the distinction of the different population of mono- and bidentate carbonate species, for Cu–Mg–Al mixed oxides as well as for the single oxide supports such as CeO_2 and TiO_2. On Mg- and Al-rich supports, predominantly bidentate carbonate species were formed contrary to Cu-rich systems where bidentate *and* monodentate species could be clearly identified. The base-catalyzed decomposition of diacetone alcohol was considered as a test reaction in order to determine the relative basicity of the surface of the mixed ($Cu_aMg_bAl_cO_x$) and single oxides (CeO_2, TiO_2) on a semi-quantitative level. Ceria and titania were found to exhibit considerable activity in the decomposition of diacetone alcohol. The results of the Cu-rich supports indicate that the addition of Cu to the $Mg_bAl_cO_x$ systems only leads to a small decrease in surface basicity.

A strong dependence of the catalytic performance on both the Cu content and the (Mg + Cu)/Al ratios was found: catalysts with a high Cu content showed higher catalytic activity in the oxidation of 1-phenylethanol compared to catalysts with a high Al content. On the materials with a *high* Cu content, bidentate and monodentate carbonates were identified and these mixed oxides showed also higher activity in the decomposition of diacetone alcohol, compared to materials with a high Al content, where monodentate carbonates could not be identified. It is concluded that under the given conditions (pressure, solvent, substrate, etc.) appropriate support basicity is crucial but not sufficient for efficient gold-catalyzed aerobic oxidation of 1-phenylethanol.

Preliminary investigations regarding the influence of the gold particle size indicated that – in contrast to CO oxidation – small gold particles (ca. 2 nm) seem to be less favorable for high activity than larger ones (ca. 9 nm). However, for a final assessment concerning the particle size effect of the gold-catalyzed aerobic oxidation improved preparation methods have to be developed that allow size-controlled synthesis of gold particles with a narrow size distribution. Research towards this aim is currently pursued in our laboratory.

Acknowledgements

The authors thank Dr. Frank Krumeich for the electron microscopy investigations performed at the electron microscopy center of ETH Zurich (EMEZ), P.H. gratefully acknowledges valuable discussions with Dr. Atsushi Urakawa.

References

[1] R.C. Bartsch, Vinyl Acetate Catalyst, US Patent 4,119,567 (1976).
[2] H. Renner, G. Schlamp, D. Hollmann, H.M. Lüschow, P. Tews, J. Rothaut, K. Dermann, A. Knödler, C. Hecht, M. Schlott, R. Drieselmann, C. Peter, R. Schiele, in: H. Pelc (Ed.), 6th ed., Ullmann's Encyclopedia of Industrial Chemistry, vol. 16, Wiley–VCH, Weinheim, 2000, p. 1.
[3] G. Roscher, in: H. Pelc (Ed.), 6th ed., Ullmann's Encyclopedia of Industrial Chemistry, vol. 38, Wiley–VCH, Weinheim, 2000, p. 59.
[4] K. Sennewald, W. Voigt, H. Glaser, Process for the manufacture of vinyl acetate, US Patent 3,761,613 (1973).
[5] T. Tacke, H. Krause, H.G.J. Lansink Rotgerink, F. Daly, M. Reisinger, H. Mangold, Supported catalyst for the production of vinyl acetate monomer, US Patent 6,821,922 (2004).
[6] D.A. Buchanan, G. Webb, J. Chem. Soc., Faraday Trans. 1 (71) (1975) 134.
[7] R.P. Chambers, M. Boudart, J. Catal. 5 (1966) 517.
[8] P.A. Sermon, G.C. Bond, P.B. Wells, J. Chem. Soc., Faraday Trans. 1 (75) (1979) 385.
[9] M. Haruta, N. Yamada, T. Kobayashi, S. Iijima, J. Catal. 115 (1989) 301.
[10] M. Haruta, Nature 437 (2005) 1098.
[11] G.C. Bond, D.T. Thompson, Cat. Rev.: Sci. Eng. 41 (1999) 319.
[12] A. Haruta, Chem. Rec. 3 (2003) 75.
[13] M. Haruta, M. Date, Appl. Catal. A: Gen. 222 (2001) 427.
[14] A.S.K. Hashmi, G.J. Hutchings, Angew. Chem. Int. Ed. 45 (2006) 7896.
[15] L. Prati, M. Rossi, J. Catal. 176 (1998) 552.
[16] C. Bianchi, F. Porta, L. Prati, M. Rossi, Top. Catal. 13 (2000) 231.
[17] S. Carrettin, P. McMorn, P. Johnston, K. Griffin, G.J. Hutchings, Chem. Comm. (2002) 696.
[18] D.I. Enache, J.K. Edwards, P. Landon, B. Solsona-Espriu, A.F. Carley, A.A. Herzing, M. Watanabe, C.J. Kiely, D.W. Knight, G.J. Hutchings, Science 311 (2006) 362.
[19] D.I. Enache, D.W. Knight, G.J. Hutchings, Catal. Lett. 103 (2005) 43.
[20] S. Biella, G.L. Castiglioni, C. Fumagalli, L. Prati, M. Rossi, Catal. Today 72 (2002) 43.
[21] A. Abad, P. Concepción, A. Corma, H. García, Angew. Chem. Int. Ed. 44 (2005) 4066.
[22] P. Haider, A. Baiker, J. Catal. 248 (2007) 175.
[23] B. Kimmerle, J.D. Grunwaldt, A. Baiker, Top. Catal. 44 (2007) 285.
[24] K. Mori, T. Hara, T. Mizugaki, K. Ebitani, K. Kaneda, J. Am. Chem. Soc. 126 (2004) 10657.
[25] J.D. Grunwaldt, C. Kiener, C. Wögerbauer, A. Baiker, J. Catal. 181 (1999) 223.
[26] J.D. Grunwaldt, M. Maciejewski, O.S. Becker, P. Fabrizioli, A. Baiker, J. Catal. 186 (1999) 458.
[27] K. Okumura, K. Yoshino, K. Kato, M. Niwa, J. Phys. Chem. B 109 (2005) 12380.
[28] V. Schwartz, D.R. Mullins, W.F. Yan, B. Chen, S. Dai, S.H. Overbury, J. Phys. Chem. B 108 (2004) 15782.
[29] N. Weiher, E. Bus, L. Delannoy, C. Louis, D.E. Ramaker, J.T. Miller, J.A. van Bokhoven, J. Catal. 240 (2006) 100.
[30] J.C. Fierro-Gonzalez, B.C. Gates, Catal. Today 122 (2007) 201.
[31] J. Guzman, B.C. Gates, J. Phys. Chem. B 106 (2002) 7659.
[32] G.J. Hutchings, M.S. Hall, A.F. Carley, P. Landon, B.E. Solsona, C.J. Kiely, A. Herzing, M. Makkee, J.A. Moulijn, A. Overweg, J. Catal. 242 (2006) 71.
[33] G.C. Bond, D.T. Thompson, Gold Bull. 33 (2000) 41.
[34] V.R. Choudhary, A. Dhar, P. Jana, R. Jha, B.S. Uphade, Green Chem. 7 (2005) 768.
[35] A.C. Gluhoi, N. Bogdanchikova, B.E. Nieuwenhuys, J. Catal. 232 (2005) 96.
[36] A.C. Gluhoi, N. Bogdanchikova, B.E. Nieuwenhuys, J. Catal. 229 (2005) 154.
[37] Z. Ma, S.H. Overbury, S. Dai, J. Mol. Cat. A: Chem. 273 (2007) 186.
[38] M.M. Schubert, S. Hackenberg, A.C. van Veen, M. Muhler, V. Plzak, R.J. Behm, J. Catal. 197 (2001) 113.
[39] D.L. Feldheim, Science 316 (2007) 699.
[40] B. Hvolbæk, T.V.W. Janssens, B.S. Clausen, H. Falsig, C.H. Christensen, J.K. Nørskov, Nano Today 2 (2007) 14.
[41] N. Lopez, T.V.W. Janssens, B.S. Clausen, Y. Xu, M. Mavrikakis, T. Bligaard, J.K. Nørskov, J. Catal. 223 (2004) 232.
[42] N. Lopez, J.K. Nørskov, T.V.W. Janssens, A. Carlsson, A. Puig-Molina, B.S. Clausen, J.D. Grunwaldt, J. Catal. 225 (2004) 86.
[43] M. Mavrikakis, P. Stoltze, J.K. Nørskov, Catal. Lett. 64 (2000) 101.
[44] F. Cavani, F. Trifiro, A. Vaccari, Catal. Today 11 (1991) 173.
[45] D. Baurecht, I. Porth, U.P. Fringeli, Vib. Spectrosc. 30 (2002) 85.
[46] T. Bürgi, A. Baiker, Adv. Catal. 50 (2006) 227.
[47] A. Urakawa, T. Bürgi, A. Baiker, Chem. Eng. Sci. 63 (2008) 4902.
[48] A. Urakawa, T. Bürgi, H.P. Schläpfer, A. Baiker, J. Chem. Phys. 124 (2006).
[49] P. Käßner, M. Baerns, Appl. Catal. A: Gen. 139 (1996) 107.
[50] J.A. Lercher, C. Colombier, H. Noller, React. Kinet. Catal. Lett. 23 (1983) 365.
[51] G.W. Wang, H. Hattori, K. Tanabe, Bull. Chem. Soc. Jpn. 56 (1983) 2407.
[52] D.G. Duff, A. Baiker, P.P. Edwards, Langmuir 9 (1993) 2301.
[53] M. Haruta, Cattech 6 (2002) 102.
[54] L. Mädler, H.K. Kammler, R. Müller, S.E. Pratsinis, J. Aerosol Sci. 33 (2002) 369.
[55] L. Mädler, W.J. Stark, S.E. Pratsinis, J. Mater. Res. 17 (2002) 1356.
[56] J.K. Edwards, B.E. Solsona, P. Landon, A.F. Carley, A. Herzing, C.J. Kiely, G.J. Hutchings, J. Catal. 236 (2005) 69.
[57] G. Busca, V. Lorenzelli, Mater. Chem. 7 (1982) 89.
[58] B. Taravel, P. Delorme, G. Chauvet, V. Lorenzelli, J. Mol. Struct. 13 (1972) 283.
[59] D. Baurecht, U.P. Fringeli, Rev. Sci. Instrum. 72 (2001) 3782.
[60] T. Bürgi, A. Baiker, J. Phys. Chem. B 106 (2002) 10649.
[61] A. Urakawa, R. Wirz, T. Bürgi, A. Baiker, J. Phys. Chem. B 107 (2003) 13061.
[62] P. Haider, J.-D. Grunwaldt, R. Seidel, A. Baiker, J. Catal. 250 (2007) 313.